Title:	Experimental investigation of dowel action using advanced measurement techniques
Authors:	Pejatovic M., Muttoni A.
Published in:	14th fib International PhD Symposium in Civil Engineering
Pages:	573-580
City, country:	Rome, Italy
Year of publication:	2022
Type of publication:	Conference Paper

Please quote as:	Pejatovic M., Muttoni A., *Experimental investigation of dowel action using advanced measurement techniques*, 14th fib International PhD Symposium in Civil Engineering, Rome, Italy, 2022, 573-580.

Experimental investigation of dowel action using advanced measurement techniques

Marko Pejatović [1] and Aurelio Muttoni [2]

[1] PhD Student, [2] PhD advisor

Structural Concrete Laboratory, IBETON
School of Architecture, Civil and Environmental Engineering, ENAC,
École Polytechnique Fédérale de Lausanne, EPFL,
Station 18, EPFL, CH-1015 Lausanne, Switzerland

Abstract
Existing shear-cracked structures need to be reliably verified in order to avoid redundant interventions. Code provisions often raise shear safety and/or fatigue life concerns of the reinforcement subjected to stress concentrations due to cyclic dowel action. This paper presents an experimental investigation on dowel action under cyclic/monotonic loading based on advanced measurement techniques: Digital Image Correlation and Optical Fibres. The aim is to develop a mechanical model which allows calculating the steel stress variations on the basis of the measured crack openings and to assess existing structures which are theoretically shear-critical. The test results show a significant dependence on bar diameter, crack kinematics and crack-bar angle. Based on the test measurements, the internal forces, the deformed bar shape and the local pressure on concrete embedment are derived.

1 Introduction

Existing Reinforced Concrete (RC) structures with shear-induced cracks (Fig.1a) need to be assessed in a reliable and an expeditious manner to avoid unnecessary repairs or to prioritise interventions in case of needed maintenance.

Verification of structural safety based on crack evolution does not necessarily imply sufficient structural capacity even in the case of small crack openings, particularly for brittle failure modes such as shear failure [1]. However, this issue can be overcome by conducting a thorough study of shear cracks which allows one to measure the crack geometry and the kinematics, to calculate the local internal forces [2], [3] and to compare them with the structural resistance. On the same basis, it is possible to estimate the stress variation and thus the cumulative fatigue damage of the reinforcement. One source of the stress variation is local bending of the reinforcement crossing active shear cracks due to cyclic dowel action caused by traffic loads, varying temperature, etc.

Code provisions [4]–[6] are in some cases overly conservative, underestimating the shear resistance and/or suggesting insufficient fatigue life of longitudinal and shear reinforcement subjected to dowel action crossing the shear cracks (Fig.1b).

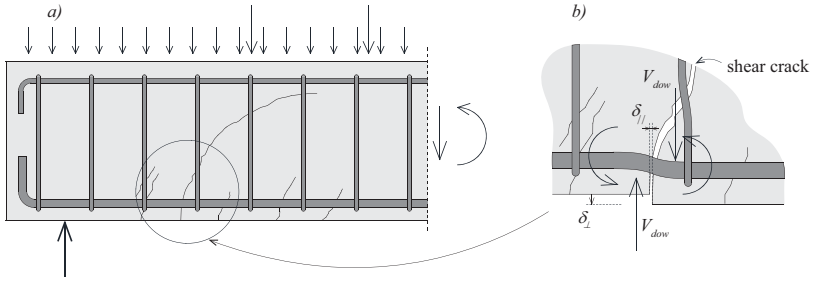

Fig.1 (a) Concrete girder with existing shear cracks and (b) local dowel mechanism of the longitudinal reinforcement and the stirrup at the crack intersection.

Most studies in the past have focused on dowel action at its ultimate stage under monotonic or large cyclic loads. The former typically leads to the dowel bar yielding due to flexion followed by local

crushing of the concrete embedment under dowel bar [7]–[12] provided that splitting and cover spalling are prevented. The latter usually causes a dowel response with degrading stiffness after several reversals due to yielding of the dowel bar and local concrete crushing [13], [14]. Dowel action under large shear displacements exerting significant catenary action has also been observed [15]. However, refined knowledge on dowel action, in terms of its contribution to carrying shear forces at all load levels and the stress variations potentially leading to the fatigue failure, is still needed.

To that aim, this paper presents an experimental investigation on dowel action due to monotonic and cyclic loading using advanced measurement techniques such as Three-Dimensional Digital Image Correlation (3D DIC) [16] and Distributed Optical Fibres (DOF) [17], [18]. They enable refined measurements of the full 3D displacement field of the cracked concrete surface and the continuous strain distribution on the steel surface, respectively. Using a custom-tailored test set-up, a series of block-type concrete specimens is subjected to low-stress level cycles and/or monotonic loading up to the final dowel rupture at the peak of catenary action. Imposed test crack kinematic parameters (opening and sliding) are chosen to correspond to the representative loading cases in practice.

2 Experimental set-up and specimens

The experimental set-up (Fig.2a) consists of a block-type reinforced concrete specimen fixed to a custom-made machine including a rigid frame on which steel plates are mounted. The machine allows one to impose independent displacements in the two perpendicular directions: the vertical and the horizontal which correspond to the crack opening and the crack sliding direction, respectively. The crack opening ($\delta_{//}$, relative displacement between the two crack lips parallel to the bar axis) is applied by pulling the dowel bar anchored in the rigid steel plates by means of threaded bar ends. The opening is controlled by using four vertical Linear Variable Differential Transformers (LVDTs), two on each front and back side of the block. The crack sliding ($\delta_{\perp}$, relative displacement between the two crack lips perpendicular to the bar axis) is imposed by controlling a pair of horizontal LVDTs placed on each block side (Fig.2b).

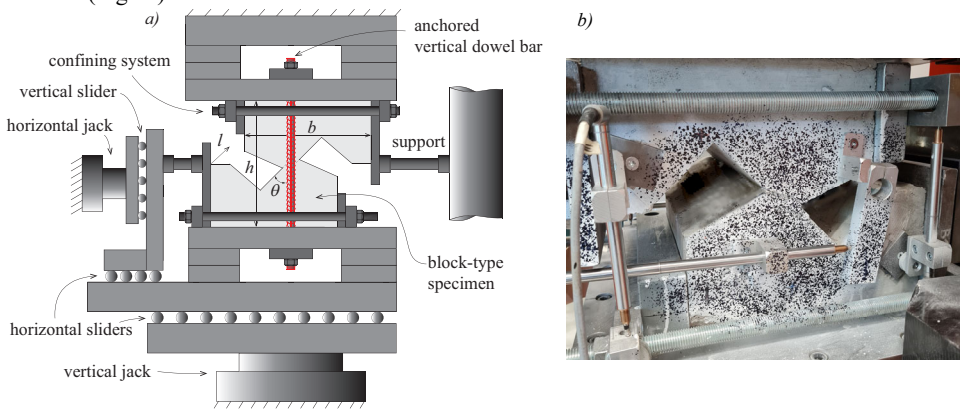

Fig.2 Test set-up: (a) front side of a specimen and (b) photo of back side of a specimen with speckled pattern for 3D DIC measurement.

Digital Image Correlation is used to measure the displacement field of the concrete surface (Fig.2b, back side of the block) in three orthogonal directions while optical fibres are glued on the dowel bar surface in order to continuously follow the strain state.

To align both horizontal forces, a rigid confining system, consisting of steel plates and ties, is used (Fig.2a). As a consequence, the rotation of the blocks is minimised.

The specimens are made of a vertical dowel bar embedded in the two reinforced concrete blocks ($b = h = l = 300$ mm) separated by a notch (Fig.2a). The dowel bar is always encased in a relatively thin cylindrical concrete layer at the bar-notch intersection to ensure a realistic crack kinematics and to avoid stress transmission by aggregate interlock. The geometry of the specimens is defined by a crack-bar angle (θ, Fig.2a) which takes the value between 45° and 90° range. The properties of the specimens are summarized in Table 1.

Table 1 Properties of the tested specimens.

Specimen	θ [°]	$Ø_s$ [mm]	f_{cm} [MPa]	f_{sy} [MPa]	cyclic / monotonic
DP2001	90	20	33.63	523.5	monotonic
DP2007	70	20	37.30	523.5	monotonic
DP2008	45	20	38.26	523.5	monotonic
DP1411	45	14	38.94	510.3	monotonic
DP2013	90	20	32.95	923.3	cyclic
DP2014	45	20	33.18	923.3	cyclic

The properties are given in terms of crack-bar inclination (θ), dowel bar diameter ($Ø_s$), mean concrete compressive strength (f_{cm}) and yield strength of the dowel bar (f_{sy}).

To prevent a global splitting failure mode at large-load levels, the blocks are reinforced by stirrups.

3 Experimental programme and test results

3.1 Monotonic tests

The specimens are subjected to two types of displacement-controlled tests: monotonic and cyclic test protocols. Fig.3c shows two different possibilities of conducting the monotonic protocol consisting of two phases: the first phase is referred to as Mode I (MI) in which the dowel bar is pulled to impose the specified initial crack opening ($\delta_{//0}$). In the subsequent phase, the shear displacement is applied, gradually increasing either in parallel with the opening increment (their ratio is defined by the angle α) or with the opening which is maintained constant until the end of the test (dowel rupture due to the catenary action). The first mode is referred to as Mixed Mode (MM) and the second as Mode II (MII).

Fig.3a shows the results of the monotonic tests in terms of shear stress in the dowel bar (V_{dow} / A_s, where V_{dow} is the shear force carried by the dowel bar and A_s is the dowel cross-section area) as a function of the imposed crack sliding ($\delta_{\perp}$) for three specimens with varying crack-bar angle (θ).

The dowel response consists in a linear-elastic domain until the stresses in the dowel bar attain its yield strength and/or concrete crushing, under the local dowel contact pressure, which softens the response. For normal strength concrete and steel, the ultimate dowel response is typically followed by both phenomena occurring simultaneously. As the dowel bar is anchored at the extremities, it is possible to further increase the shear force due to second order effects of the axial tensile force in the dowel bar (catenary action) which becomes significant when the sliding displacement is large. Eventually, the tests typically terminate with the dowel bar fracture close to the crack where the maximum stresses caused by the combination of flexion and tension can be observed.

Three specimens with the same bar diameter (20 mm), imposed crack kinematics ($\delta_{//0} = 0.2$ mm, $\alpha = 0°$) with varying crack-bar angle (45°, 70° and 90°) have been tested under the monotonic test protocol. Specimens DP2001 and DP2007 failed with a catenary fracture while specimen DP2008 had a premature failure of the anchorage thread. The results show that the ultimate dowel resistance strongly depends on the crack inclination. Larger crack-bar angles provide stronger support to the dowel bars limiting concrete cracking and crushing. Analogously, the initial stiffness of the response curve decreases for smaller crack-bar angles (Fig.3b).

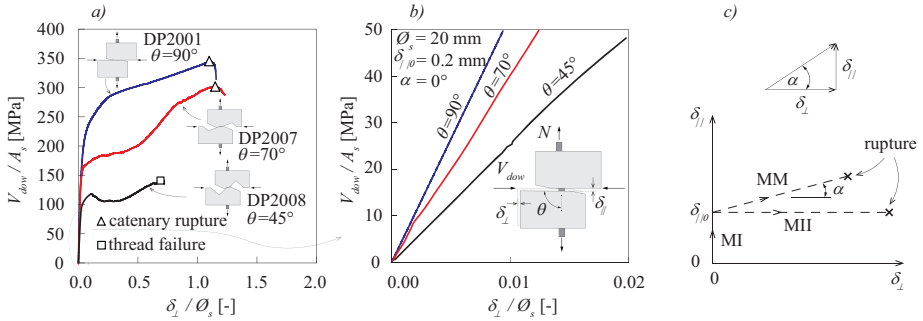

Fig.3 Monotonic tests: (a) dowel response in terms of shear stress as a function of shear sliding of three specimens ($Ø_s$ = 20mm) with varying crack-bar angle; (b) initial stiffness and (c) scheme of the monotonic test protocol.

Fig.4 presents the influence of the bar dimeter ($Ø_s$ = 14 mm, 20 mm) on the full shear stress-sliding response of the dowel bar under the monotonic loading protocol. On this basis, the normalized resistance shown in Fig.4a seems to be similar for both tests (at least up to the premature failure of the threaded-end anchorage of the test with $Ø_s$ = 20 mm) whereas the initial stiffness seems to be higher for the larger bar diameter (Fig.4b).

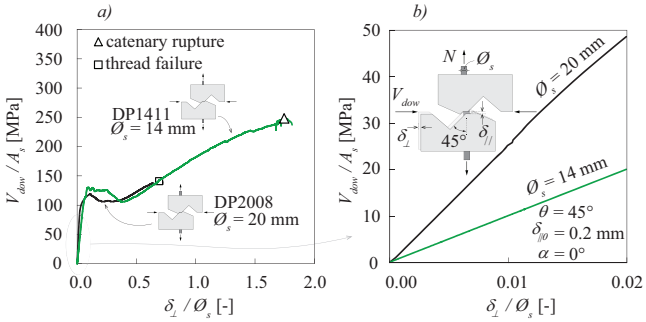

Fig.4 Monotonic tests: (a) dowel response in terms of shear stress in the function of shear sliding of two specimens (θ = 45°) with varying bar diameter and (b) initial stiffness.

3.2 Cyclic tests

The cyclic tests are carried out in three phases (see Fig.5b). Once the crack has been opened to its initial values (Mode I), a specified sliding is imposed in the second phase (Mode II). As observed in typical shear tests on reinforced concrete members, these two imposed kinematic components provide a realistic initial loading condition on the dowel bar [2], [3]. Finally, various cyclic crack kinematics, causing elastic stresses both in concrete and steel, are applied in the third phase.

Fig.5a shows the cyclic test results (different colour shades refer to distinctive applied crack kinematics) for two specimens with various crack inclinations and are compared to the corresponding monotonic tests. It can be observed that the comparable test responses under cyclic and monotonic loading regimes are similar in terms of stiffness.

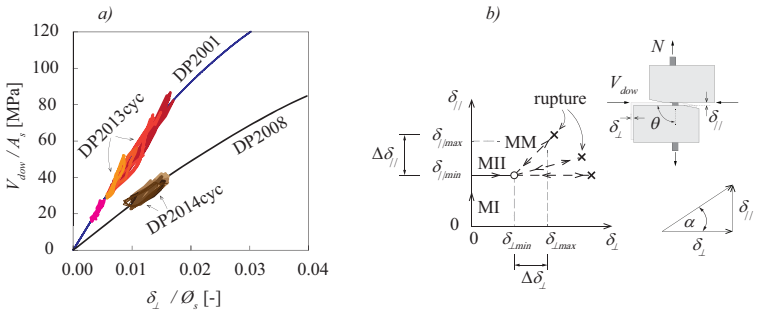

Fig.5 Cyclic tests: (a) cyclic responses (colour shades) due to various imposed kinematics in terms of shear stress in the dowel bar as a function of shear sliding of two specimens with varying crack-bar angle compared with the monotonic tests and (b) scheme of the cyclic test protocol.

Optical fibres glued on both sides of the dowel bar (Fig.6a) on a surface in a groove enable the continuous measurement of the strains along the rebar (Fig.6b). Based on the measured strains, the internal forces, the contact pressure on the surrounding concrete as well as the dowel bar deformation corresponding to the crack sliding are derived for the case of an inclined-crack specimen (DP2014cyc) subjected to cyclic displacements with the imposed kinematics of minimum/maximum crack sliding $\delta_{\perp min/max} = 0.24/0.31$ mm and opening $\delta_{//min/max} = 0.1/0.14$ mm (Fig.6).

Internal forces (axial force (N), bending moment (M) and dowel force (V_{dow})) in the dowel bar are normalized in terms of their corresponding stress components: the average axial stress $\Delta\sigma_{s,\,avg} = N / (\pi \cdot \varnothing_s^2/4)$ (Fig.6c), the axial stress at the bar edge cause by flexion $\Delta\sigma_{s,\,flex} = M / (\pi \cdot \varnothing_s^3/32)$ (Fig.6d) and the average shear stress $\tau_s = V_{dow} / (\pi \cdot \varnothing_s^2/4)$ (Fig.6e). The average axial stress attains the value of around 150 MPa, whereas the axial stress due to flexion reaches the maximum value near to 200 MPa. The pressure on the concrete embedment is around 25 MPa ($\sim 0.76 \cdot f_{cm}$) with a slight variation due to the cyclic loading.

The curvature is calculated based on the measured strains as

$$\kappa = \frac{\varepsilon_s + \varepsilon_n}{d_f}, \tag{1}$$

where ε_s and ε_n refer to strain measured by a fibre glued on both sides while d_f refers to the distance between the two fibres which is slightly smaller than the bar diameter because the fibres are laid inside the groove along the bar.

The deformation of the bar corresponding to the sliding ($\delta_\perp$, zero rotations at the extremities, Fig.6i) is derived by integrating the rotation distribution (Fig.6h) from which the non-sliding-induced rotations have been eliminated:

$$\delta_\perp = \int \psi_{\delta_\perp} dy \tag{2}$$

The deformed shape derived from the optical fibre measurements (solid line, Fig.6i) is compared with the sliding measured by DIC (dashed line, Fig.6i). The former is slightly smaller due to the inability of the fibres to capture shear strains in the reinforcement bar. The maximum total strain variation in this case is $\Delta\varepsilon_{n,\,max}$.

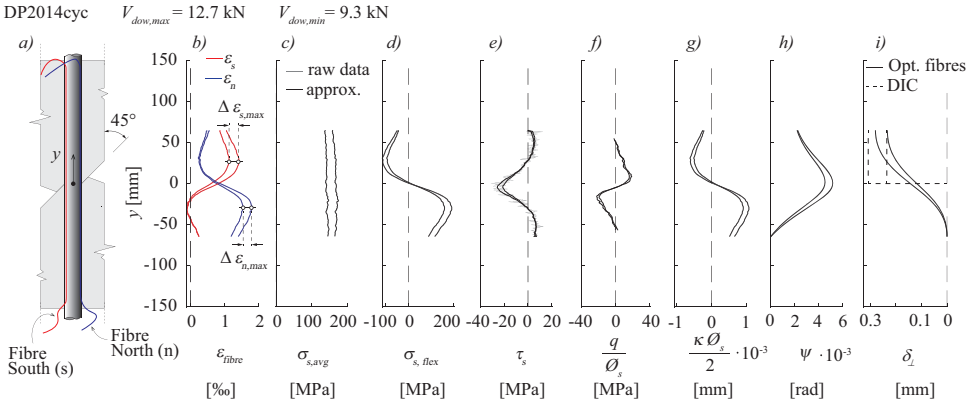

Fig.6 Results based on the optical fibre measurements with a smooth dowel bar: (a) optical fibres glued on the groove surface; (b) measured strains and (c-i) derived parameters.

Fig.7a shows the results of a cyclic test in terms of the relationship between the crack kinematic and the two axial stress components ($\Delta\sigma_{s,\,avg}$ and $\Delta\sigma_{s,\,flex}$, Fig.7b), at the location of the maximum total strain variation (in this case, the strain variation $\Delta\varepsilon_{n,\,max}$ which is located around 30 mm (~1.5$\varnothing_s$) from the crack, Fig.6b) for specimen DP2014. The dowel bar is subjected to a three-phase regime including the crack opening in Mode I, shearing the bar in Mode II and cyclic Mixed-Mode in which the total stress variation is measured. It can be observed that during the Mixed-Mode (for a given crack inclination, dowel bar diameter and crack kinematics, specimen DP2014), the bar sustains the maximum total stress variation of around 60 MPa.

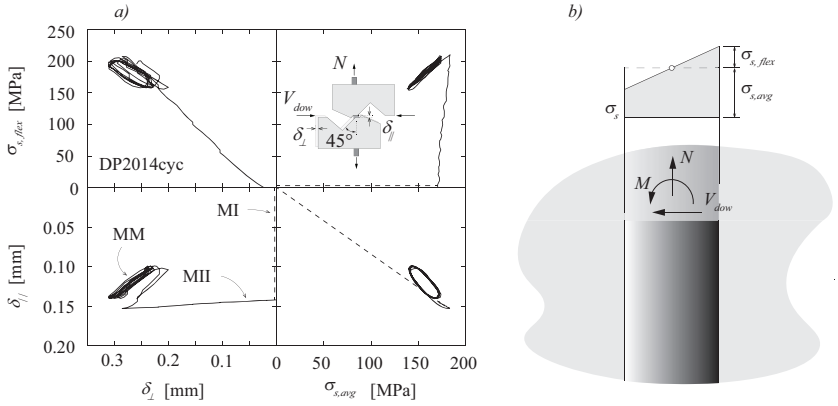

Fig.7 Results of a cyclic test: (a) relationship between the crack kinematic and the normal stress components in Mode I, Mode II and Mixed-Mode and (b) scheme of axial and flexural normal stress components.

4 Theoretical outlook

The experimental findings based on the optical fibre measurements in terms of concrete pressure on the dowel bar (Fig.8a) are intended to be used to develop a mechanical model to predict the internal forces of the dowel bar (axial, shear force and bending moment, Fig.8b) and the steel stress variations as a function of the measured or calculated crack kinematics (crack opening and crack sliding, Fig.8c). Also, the model is conceived to allow estimating the deformed bar shape once the internal forces are known.

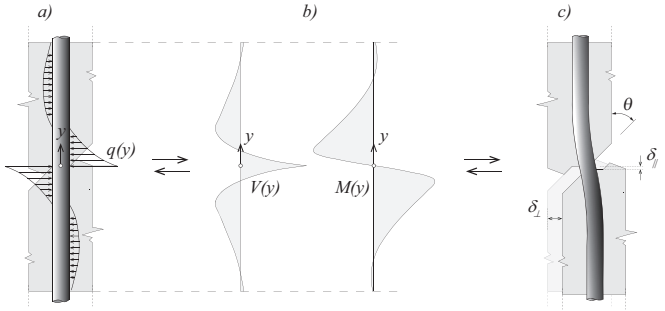

Fig.8 The outlook of the research purposes based on the experimental findings obtained using the advanced measurements in terms of (a) concrete pressure; (b) internal forces and (c) deformation of the dowel bar.

The calculation of the steel stresses and the stress variations based on the displacements measured on the concrete surface will allow verifying the fatigue resistance of existing reinforced concrete structures based on health monitoring also in cases where the reinforcement bars are not directly instrumented (this is particularly useful, since instrumenting bars in existing structures significantly disturb the bond and dowel behaviour of the reinforcement).

5 Conclusions

This paper presents an experimental investigation of dowel action based on advanced measurement techniques for dowel tests with varying crack-bar angle, bar diameter and imposed crack kinematics. The following conclusions can be drawn:

- Two different types of tests are carried out: monotonic and cyclic tests. The cyclic tests are consistent with the monotonic tests in terms of the dowel response, without noticeable stiffness degradation due to the imposed low-stress cyclic regime.
- The measured dowel response highly depends on the applied crack kinematics, on the inclination of the crack with respect to the reinforcement bar and on the diameter of the dowel bar.
- The test results systematically show that the dowel response is both stronger and stiffer for increasing crack-bar angle. The explanation of this trend lays in stronger and stiffer concrete embedment.
- Distributed optical fibre measurements show that the maximum total stress variation due to the cyclic loading is approximately located at the distance $1.5Ø_s$ from the crack.

References

[1] Zaborac J., Athanasiou A., Salamone S., Bayrak O., and Hrynyk T. 2018. “Evaluation of Structural Cracking in Concrete: Final Report (FHWA 0-6919-1),” [Online]. Available: http://library.ctr.utexas.edu/ctr-publications/0-6919-1.pdf

[2] Cavagnis F., Fernández Ruiz M., and Muttoni A. Nov. 2015. “Shear failures in reinforced concrete members without transverse reinforcement: An analysis of the critical shear crack development on the basis of test results,” Engineering Structures, vol. 103, pp. 157–173, doi: 10.1016/j.engstruct.2015.09.015.

[3] Cavagnis F., Fernández Ruiz M., and Muttoni A. Feb. 2018. “An analysis of the shear-transfer actions in reinforced concrete members without transverse reinforcement based on refined experimental measurements,” Structural Concrete, vol. 19, no. 1, pp. 49–64, doi: 10.1002/suco.201700145.

[4] “Eurocode 2: Design of concrete structures-Part 1-1: General rules and rules for buildings,” 2004.

[5] Fédération internationale du béton., Fib Model Code 2010 for concrete structures. 2010.

[6] "SIA 262:2013 - Structures en béton, Zurich, Switzerland: Société suisse des ingénieurs et des architectes," 2013. [Online]. Available: www.sia.ch/correctif.
[7] Rasmussen H. B. 1963. "Betonindstøbte, tværbelastede boltes og dornes bæreevne." Bygningsstatiske Meddelelser (in Danish), vol. 34, no. 2.
[8] Soroushian P., Obaseki K., Rojas M. C., and Sim J. 1986. "Analysis of Dowel Bars Acting Against Concrete Core,".
[9] Dulacska H. 1972. "Dowel Action of Reinforcement Crossing Cracks in Concrete." pp. 754–757.
[10] Harrild J. S. P. 2017. "Design and Modeling of Structural Joints in Precast Concrete Structures.". PhD diss., Technical University of Denmark.
[11] Dei Poli S., Di Prisco M., and Gambarova P. G. 1992. "Shear Response, Deformations, and Subgrade Stiffness of a Dowel Bar Embedded in Concrete.".
[12] Dei Poli S., Di Prisco M., and Gambarova P. 1988. "In tema di trasmissione del taglio negli elementi di calcestruzzo armato Alcuni risultati sperimentali attinenti alla cosidetta azione di spinotto.".
[13] Vintzeleou E. N. and Tassios T. P. 1987. "Behavior of Dowels under Cyclic Deformations.".
[14] Vintzēleou E. N. and Tassios T. P. Mar. 1986. "Mathematical models for dowel action under monotonic and cyclic conditions." Magazine of Concrete Research, vol. 38, no. 134, pp. 13–22, doi: 10.1680/macr.1986.38.134.13.
[15] Sørensen J. H., Hoang L. C., Olesen J. F., and Fischer G. Aug. 2017. "Testing and modeling dowel and catenary action in rebars crossing shear joints in RC." Engineering Structures, vol. 145, pp. 234–245, doi: 10.1016/j.engstruct.2017.05.020.
[16] Nonis C., Niezrecki C., Yu T.-Y., Ahmed S., Su, C.-F. and Schmidt T. Apr. 2013. "Structural health monitoring of bridges using digital image correlation." p. 869507. doi: 10.1117/12.2009647.
[17] Bado M. F. and Casas J. R. Mar. 01, 2021. "A review of recent distributed optical fiber sensors applications for civil engineering structural health monitoring." Sensors, vol. 21, no. 5. MDPI AG, pp. 1–83, doi: 10.3390/s21051818.
[18] Lemcherreq Y., Galkovski T., Mata-Falcón J., and Kaufmann W. Mar. 2022. "Application of Distributed Fibre Optical Sensing in Reinforced Concrete Elements Subjected to Monotonic and Cyclic Loading." Sensors, vol. 22, no. 5, doi: 10.3390/s22052023.